Archive of Applied Mechanics (2021) 91:3151–3170
https://doi.org/10.1007/s00419-021-01957-7

ORIGINAL

Jeremiah J. Rushchitsky

Scenarios of evolution of some types of simple waves in nonlinear elastic materials

Received: 19 October 2020 / Accepted: 8 April 2021 / Published online: 28 April 2021

Abstract Four differing from each other scenarios of evolution of the plane and close to them cylindrical solitary (simple) waves are established and commented. The material of propagation of waves is assumed to be elastic, the nonlinear deformation of which is described by the five-constant Murnaghan model (potential). The initial wave profile is given by the cosinusoidal, Gauss, Whittaker, Macdonald functions. The scenarios for the cosinusoidal (harmonic) profile are used as the classical and reference one. The methods of successive approximations and restriction on the gradient of displacement are utilized. A novelty in the description of scenarios is that the first three approximations are taken into account. This changes essentially the known (based on the first two approximations) scenarios and exposes some new wave effects. The similarities and distinctions of the presented four scenarios are commented. For example, the initial stages and effect of forming the asymmetric profile are quite similar to both the asymmetric and symmetric initial profiles. But also the scenarios show the transition from the one-hump profile to the two-hump or three-hump ones. Some of the scenarios show the drift of the profile relative to the horizontal axis. A row of other features of scenarios is commented.

Keywords Simple (solitary) wave · Scenario of evolution · Effect of third approximation

1 Introduction

There are different definitions of simple waves starting with the famous work of Riemann [1] and finishing with the works of Lighthill [2], Whitham [3], and Maugin [4, 5].

One of the definitions is as follows [5, 6]: the wave of displacement $u(x,t)$ is the simple one if its mathematical representation has simultaneously the simplest form of the solitary wave (the initial wave profile is defined by the finite function $F(x)$) and the D'Alembert wave $F(x-vt)$ ($\sigma = x - \mathrm{vt}$ is the wave phase), in which the wave velocity v depends on the gradient displacement $v = v\left(u_{,x}\right)$.

Just such kind of waves is studied in the proposed below work. The initial profiles are chosen in the form of Gauss, Whittaker, Macdonald functions. The medium of propagation is chosen as the quadratic nonlinear elastic materials which are described by the five-constant Murnaghan elastic potential [6].

The Murnaghan potential is expressed through the nonlinear Cauchy-Green strain tensor

$$\varepsilon_{\mathrm{nm}} = \left(1/2\right)\left(u_{n,m} + u_{m,n} + u_{k,n}u_{k,m}\right) \tag{1}$$

and has the form

$$W(\varepsilon_{ik}) = \left(1/2\right)\lambda(\varepsilon_{\mathrm{mm}})^2 + \mu(\varepsilon_{ik})^2 + \left(1/3\right)A\varepsilon_{ik}\varepsilon_{\mathrm{im}}\varepsilon_{\mathrm{km}} + B(\varepsilon_{ik})^2\varepsilon_{\mathrm{mm}} + \left(1/3\right)C(\varepsilon_{\mathrm{mm}})^3 \tag{2}$$

J. J. Rushchitsky (✉)
SPTimoshenko Institute of Mechanics, Kyiv, Ukraine
e-mail: rushch@inmech.kiev.ua

Thus, this potential includes quadratic and cubic summands and is characterized by five elastic constants $\lambda,\ \mu,\ A,\ B,\ C$. Correspondingly, the constitutive equations (which express the components of the symmetric Lagrange stress tensor σ_{ik} through the components of the strain tensor (1)) are quadratic nonlinear relative to the strain tensor.

Note that the elastic potentials have always the order of nonlinearity one more than the constitutive equations. Therefore, the quadratic nonlinear potential generates the linear elastic model (Hooke model), the cubic nonlinear potential generates the quadratic nonlinear elastic model, and so on.

It is worthy to note that the Murnaghan model has a big advantage as compared with other nonlinear models of elastic deformation—all set of elastic constants of this model is determined for a lot of numbers of real engineering materials (from tens types of the steel, aluminum, copper to the different plastics) [7–9].

The potential (2) can be written relative to the nine gradients of displacements $u_{i,k}$ and then this potential is expressed through summands of five different orders (from the second order to the sixth one). The classical approach consists in saving only the quadratic and cubic nonlinear summands [10–12]

$$W = (1/2)\lambda(u_{m,m})^2 + (1/4)\mu(u_{i,k} + u_{k,i})^2 + (\mu + (1/4)A)u_{i,k}u_{m,i}u_{m,k} + (1/2)(\lambda + B)u_{m,m}(u_{i,k})^2 + (1/12)Au_{i,k}u_{k,m}u_{m,i} + (1/2)Bu_{i,k}u_{k,i}u_{m,m} + (1/3)C(u_{m,m})^3. \tag{3}$$

To write the corresponding constitutive equations, another ordered pair is used—(the nonsymmetric Kirchhoff stress tensor t_{nm}, the gradients of displacements $u_{i,k}$).

Very often, the case is considered when the motion occurs in the direction of the abscissa axis and the dis-placements have the form $u_k = u_k(x_1, t)$. Then the potential (3) is simplified [10–12]

$$W = (1/2)\left[(\lambda + 2\mu)(u_{1,1})^2 + \mu\left[(u_{2,1})^2 + (u_{3,1})^2\right]\right] + \\ + \left[\mu + (1/2)\lambda + (1/3)A + B + (1/3)C\right](u_{1,1})^3 + (1/2)(\lambda + B)u_{1,1}\left[(u_{2,1})^2 + (u_{3,1})^2\right] \tag{4}$$

If to narrow the analysis to the plane waves, then the potential (4) generates the quadratic nonlinear wave equations. Later, the analysis is concentrated on the longitudinal waves which are described by the equation

$$\rho u_{1,tt} - (\lambda + 2\mu)\, u_{1,11} = N_1\, u_{1,11}u_{1,1} + N_2(u_{2,11}u_{2,1} + u_{3,11}u_{3,1}); \tag{5}$$

$$N_1 = [3(\lambda + 2\mu) + 2(A + 3B + C)]; \quad N_2 = \lambda + 2\mu + (1/2)A + B.$$

The simplest problem for the longitudinal wave is the so-called first standard problem when initially only the longitudinal wave is excited. Then the Eq. (5) is simplified to the form [10–12]

$$\rho u_{1,tt} - (\lambda + 2\mu)\, u_{1,11} = N_1\, u_{1,11}u_{1,1} \to u_{1,tt} - (c_L)^2\, u_{1,11} = (N_1/\rho)\, u_{1,11}u_{1,1}, \tag{6}$$

where $c_L = \sqrt{(\lambda + 2\mu)/\rho}$ is the constant phase velocity of a longitudinal wave in the linear approach.

An analysis of the nonlinear harmonic waves as a solution of the Eq. (6) belongs to the classical one. Three methods mainly are utilized—the method of successive approximations, the method of slowly varying amplitudes, the method of restrictions on the gradient of displacement.

It should be noted that the nonlinear wave equation of the type (6) occurs not only in mechanics. The corresponding optic waves were studied by Bloembergen [13], and his results were awarded by the Nobel Prize in physics of 1980 (for his contribution to the development of laser spectroscopy). These results include the description of the transformation of the initial harmonic (the beam of the ruby laser in the form of the red light with the wavelength of 6940) into the second one (blue light with the wavelength of 3470) when the light propagates through the crystal of potassium dihydro phosphate KH_2PO_4 [14].

Roughly speaking, the main wave effect for this kind of wave in different areas of modern physics (optics, radiophysics, acoustics, mechanics, etc.) is the generation of the 2nd harmonic owing to the self-generation of the 1st harmonic. Usually, this effect is described analytically by the method of slowly varying amplitudes, which shows the final result (the 1st harmonic at the entrance and the 2nd harmonic at the outlet) and the scenario of transition from the entrance to the outlet cannot be seen.

A possibility of seeing the scenario of the wave evolution gives the method of successive approximation. It proposes the simple approximate analytical formulas which show the step-by-step change the initial profile of the wave. The features of the scenario are exposed most clearly in numerical modeling. Because the problem

is the multi-parameter one, the progress of the wave evolution depends essentially on the choice of material, wavelength, initial amplitude of the wave.

The method of successive approximations is also called the perturbation method or the method of a small parameter. The main feature of this method is the introduction of a small parameter ε [10].

Consider further the nonlinear wave Eq. (6). According to this method, the function $u(x_1, t, \varepsilon)$ is chosen and represented in the form of a convergent series

$$u(x_1, t, \varepsilon) = \sum_{n=0}^{\infty} \varepsilon^n u^{(n)}(x_1, t) = u^{(0)}(x_1, t) + \varepsilon u^{(1)}(x_1, t) + \varepsilon^2 u^{(2}(x_1, t) + \cdots \tag{7}$$

The zeroth term $u^{(0)}(x_1, t)$ is assumed to be the solution of the corresponding to (6) linear wave equation

$$u_{1,tt} - (c_L)^2 \, u_{1,11} = 0 \tag{8}$$

Note that a necessary condition of this method is the existence of the linear part of the nonlinear equation.

Basing on representation (7), the solution of nonlinear Eq. (6) is sought in the form of successive approximations

$$u(x_1, t) = u(x_1, t, \varepsilon = 1) = \sum_{n=0}^{\infty} u^{(n)}(x_1, t) = u^{(0)}(x_1, t) + u^{(1)}(x_1, t) + u^{(2}(x_1, t) + \cdots \tag{9}$$

A feature of this method is that the arbitrary approximation $u^{(n)}(x_1, t)$ is found as the solution of inhomogeneous linear equation

$$u^{(n)}_{1,tt} - (c_L)^2 \, u^{(n)}_{1,11} = \left(N_1 / \rho\right) u^{(n-1)}_{1,11} u^{(n-1)}_{1,1} \tag{10}$$

This means that to find the n-th approximation, it is necessary to know only the $(n-1)$-th approximation and solve only the inhomogeneous linear wave equation with the known right-side term.

This method works well in the theory of waves, when the initial amplitude doesn't increase essentially (in some cases, half as much again).

Further, an analysis of each kind of wave contains the theoretical and numerical parts. The theoretical part involves the statement of the problem in terms of the nonlinear theory of elasticity and description of the procedure of the approximate method of solving the problem that uses the 1st, 2nd, and 3rd approximations. In contrary to the classical approach that utilizes the 1st and 2nd approximations only, the using of the 3rd approximation permits to show the scenarios of evolution of the wave more in detail and detect some new nonlinear wave effects.

2 Classical scenarios of the evolution of wave with harmonic profile

Consider now the plane longitudinal elastic wave within of framework of its description by the nonlinear wave Eq. (6). Let the wave is a harmonic one. Then the initial wave profile is defined by the formula

$$u_1(x_1, t = 0) = u_{1o} \cos k_L x_1, \tag{11}$$

where u_{1o} and k_L are the initial wave amplitude and the wave number, respectively.

It is assumed that the initial impulse of the profile (11) generates the harmonic wave with the frequency ω and phase $\sigma = k_L x_1 - \omega t$

$$u_1(x_1, t) = u_{1o} \cos(k_L x_1 - \omega t) = u_{1o} \cos \sigma \tag{12}$$

Apply now the method of successive approximations to the Eq. (6). This approach was realized before for different levels od approximations (first two, first three, first four, etc.) [10, 15–19].

The zeroth approximation $u^{(0)}_1(x_1, t)$ corresponds to the Eq. (8) and has the form (12).

The 1st approximation $u^{(1)}_1(x_1, t)$ is a solution of the inhomogeneous linear wave equation

$$u^{(1)}_{1,tt} - (c_L)^2 u^{(1)}_{1,11} = \left(N_1 / \rho\right) u^{(0)}_{1,11} u^{(0)}_{1,1} \tag{13}$$

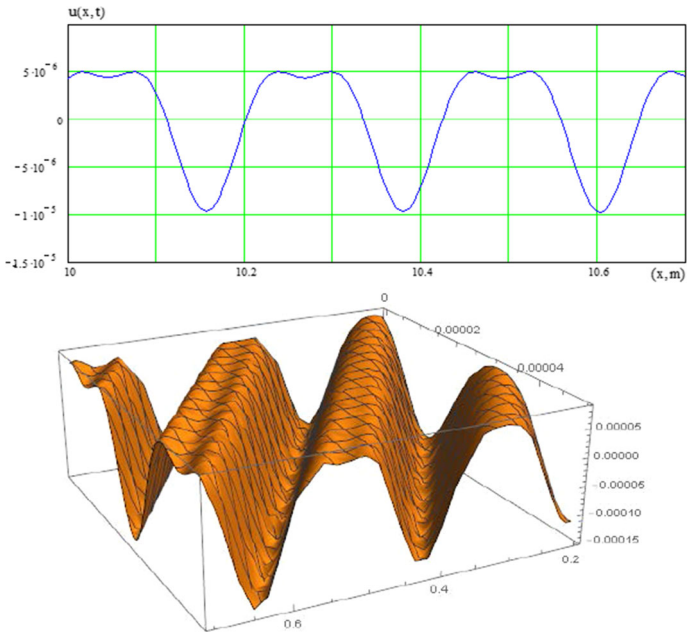

Fig. 1 Evolution of the initial harmonic profile in coordinates "distance of propagation—displacement" (2D picture) and– in coordinates "time of propagation—a distance of propagation—displacement" (3D picture)

and has the form [9–11]

$$u_1^{(1)}(x_1, t) = x_1 \left[\frac{N_1}{8(\lambda + 2\mu)} (u_{1o})^2 k_L^2 \right] \cos 2\sigma. \tag{14}$$

If two first approximations are saved, then the approximate solution consists of the sum of two harmonics [8]

$$u_1^{0+1}(x_1, t) = u_1^{(0)}(x_1, t) + u_1^{(1)}(x_1, t) = u_{1o} \cos\sigma + x_1 \left[\frac{N_1}{8(\lambda + 2\mu)} (u_{1o})^2 k_L^2 \right] \cos 2\sigma \tag{15}$$

The solution (15) confirms theoretically a generation of the 2nd harmonic. It describes the classical scenario of the evolution of initially harmonic wave (12)—owing to the mechanism of self-generation, the 1st harmonic is transformed with increasing the time of propagation (or with increasing the distance of propagation) into the 2nd harmonic.

This scenario (scenario cos + 0 + 1) is the same for a different choice of initial parameters (initial amplitude, frequency, elastic material constants) on the whole, but the different choice of parameters changes the distan ce, on which the scenario is realized fully.

The characteristic dependence of the amplitude of wave on the time and distance of its propagation is shown in Fig. 1.

The 2D picture shows an evolution in coordinates "distance of propagation—displacement", and the 3D picture—in coordinates "time of propagation—a distance of propagation—displacement".

The Figs. 2, 3, 4, 5 show consequently the mentioned above stages. Because the scenario cos + 0 + 1 is probably the most studied before, then below the stages of evolution are shown more in detail in 2D pictures [10]. This scenario is divided into four stages.

Stage 1. The initial harmonic profile tilts downwards under the constant angle, i.e., the maximal positive values decrease, and the maximal negative values increase. On this faintly developed stage, the profile is transformed from the harmonic one into not harmonic, but very close to harmonic profile. This stage is shown in Fig. 2.

Stage 2. The tops of the profile get lower, and the plateaus are gradually formed instead of the peak. Later the plateau lowers even more, the middle part of the plateau begins to sag, and the profile becomes two-humped instead of one-humped. The frequency of repetition of the same profile does not change.

This poorly and later intermediately developed stage of evolution is shown in Figs. 3 and 4.

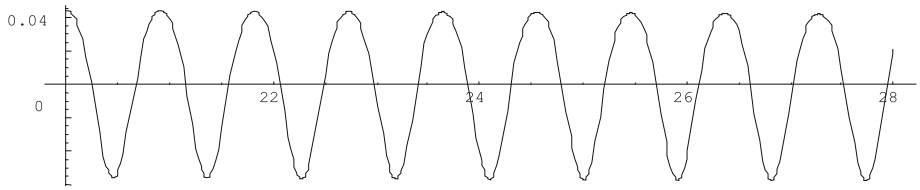

Fig. 2 Scenario cos + 1 + 2. Stage 1

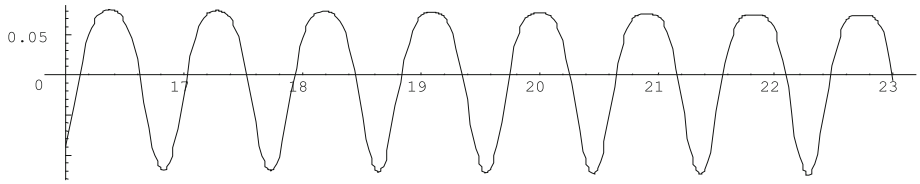

Fig. 3 Scenario cos + 1 + 2. Stage 2

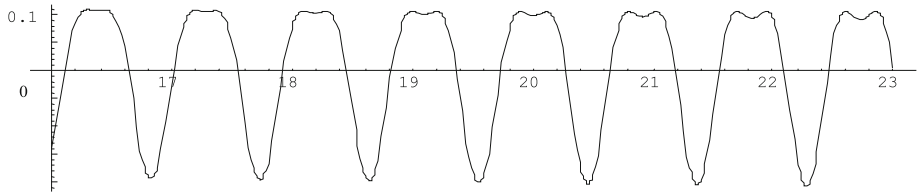

Fig. 4 Scenario cos + 1 + 2. Stage 2

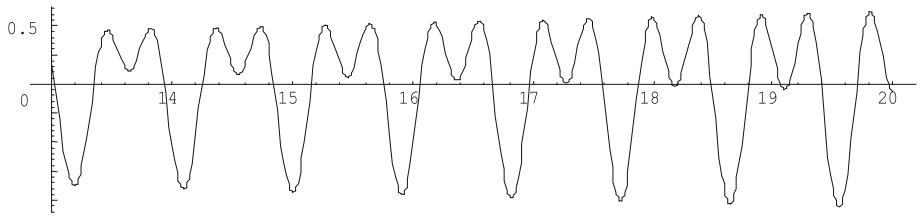

Fig. 5 Scenario cos + 1 + 2. Stage 3

Stage 3. Saving the prior frequency, the profile becomes more clearly two-humped with an increasing sag up to the point when it touches the abscissa axis. This stage is shown in Fig. 5.

Stage 4. The sag increases, and the profile becomes similar to the harmonic one with the 2nd harmonic frequency but with the unequal amplitude swings: upwards—the large amplitude, downwards—roughly half the size of the prior one, upwards—slightly bigger than the prior upper one, downwards—roughly twice as big as the prior lower one. So, the gradual change (progress) of the 1st harmonic profile transforms it into the 2nd harmonic profile and the transformation of 1st harmonic into the 2nd one can be observed. This stage is shown in Fig. 6.

It was found that the notation

$$M = \frac{N_1}{8(\lambda + 2\mu)} u_{1o}(k_L)^2 = \frac{1}{8\rho} N_1 u_{1o} \frac{k_L^2}{v_L^2} = \frac{1}{8\rho} N_1 u_{1o} \frac{\omega^2}{v_L^4} \tag{16}$$

is convenient in the analysis that includes the next approximations. Then solution (15) can be written in the form

$$u_1^{0+1}(x,t) = u_1^{(0)}(x_1,t) + u_1^{(1)}(x_1,t) = u_{1o}\cos\sigma + u_{1o}Mx_1\cos 2\sigma. \tag{17}$$

For many real materials, the parameter N_1 is the negative quantity and has the order $\sim 10^{12}$. The density and phase velocity have roughly the identical orders $\rho \sim 10^3 \div 10^4$, $v_{ph} \sim 10^3 \div 10^4$. If the frequencies are chosen from the ultrasound range $\omega \sim 10^4 - 10^6$, then the wavenumbers have the order $k = \left(\omega / v_{ph}\right) \sim 10 - 10^3$.

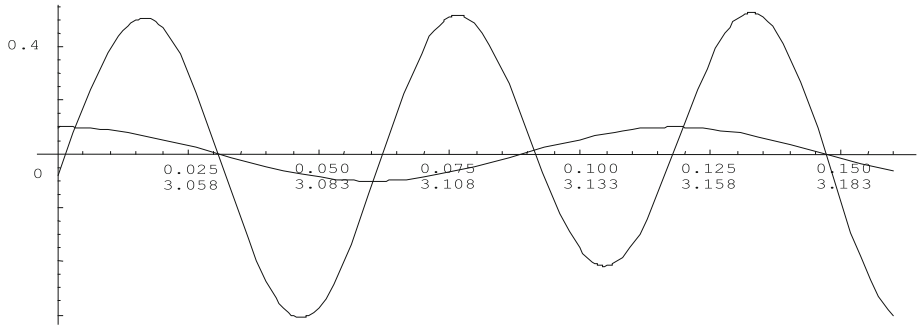

Fig. 6 Scenario cos + 1 + 2. Stage 4

They correspond to the wavelengths within the range of 1 cm−100 microns. If to assume the initial amplitude to be small one order smaller (10 times) of the wavelength, then $u_o \sim 10^{-4} - 10^{-5}$. This reasoning permits us to estimate the order of constant $M \sim 10^{-1} - 10^{-2}$.

The quantity Mx_1 gives according to (17) the relation between amplitudes of the 1st and 2nd harmonics. Hence, to small is the parameter M, to large distance is needed for describing the full scenario. This general fact means that in this context the choice of some forming the value M concrete set parameters is not important for the structure of the scenario. This choice determines only the value of the distance. The written above note is true for all scenarios shown further for different simple waves.

A feature of the presented further results is in using three approximations and comparing the new scenarios with the classical one for the harmonic wave and the observed scenarios with each other. Therefore, it is necessary to show here the solution of the nonlinear wave Eq. (6) for the first three approximations. So, the 3rd approximation is as follows [10, 15–19]

$$u_1^{(2)} = u_{1o}(M_L)^3(x_1)^3\left[-\frac{8}{3} + \frac{5}{2k_Lx_1}\sin 4\sigma + \left(-\frac{4}{3} + \frac{11}{8(k_L)^2(x_1)^2}\right)\cos 4\sigma.\right. \tag{18}$$

Thus, similarly to that as the 2nd approximation introduces into the general wave picture the 2nd harmonic, the 3rd approximation introduces additionally the 4th harmonic.

The solution within the framework of the first three approximations has the form [10]

$$u_1^{0+1+2}(x_1,t) = u_1^{(0)}(x_1,t) + u_1^{(1)}(x_1,t) + u_1^{(2)}(x_1,t) = u_{1o}\cos\sigma + u_{1o}M_Lx_1\cos 2\sigma + \\ + u_{1o}(M_L)^3(x_1)^3\left[-\frac{8}{3} + \frac{5}{2k_Lx_1}\sin 4\sigma + \left(-\frac{4}{3} + \frac{11}{8(k_L)^2(x_1)^2}\right)\cos 4\sigma\right]. \tag{19}$$

In this case, the corresponding to the first two approximation scenario cos + 0 + 1 is changed.

In the 1st stage of the scenario cos + 0 + 1 + 2, the wave is initially slightly distinguished from the linear harmonic wave. The Fig. 7 shows the initial part of wave motion for three approximations when nonlinearity is just beginning to manifest itself. Here, the 1st approximation corresponds to the top line for positive amplitude values, the 1st + 2nd and 1st + 2nd + 3rd corresponds to the bottom line for positive amplitude values.

On the 2nd stage, with an increase of the passed by wave distance or the time of wave propagation the 1st harmonic is summing up with the 2nd and 4th harmonics, and they form together the weak-modulated wave. At that, the profile saves the prior frequency and starts to be the three-humped with an increasing central hump.

This stage is shown in Fig. 8, where the 1st approximation corresponds to the top line for positive amplitude values, the 1st + 2nd—to the bottom line for positive amplitude values, and 1st + 2nd + 3rd—to the middle line for positive amplitude values.

The 3rd stage consists in that with time the effect of the 4th harmonic increases, and it becomes dominant in amplitude. But at that, the profile of the wave motion is similar to the profile of the 3rd harmonic, and most of the profile is located in the positive part of amplitudes. Thus, this stage shows some picture differing from the prior one in Fig. 8. The Fig. 9 demonstrates this difference. Here, the 1st approximation corresponds to the middle line for the positive amplitude values, the 1st + 2nd—to the bottom line for positive amplitude values, and 1st + 2nd + 3rd—to the top line for positive amplitude values.

The 4th stage shows an increasing the new wave effects from stage 3—the profile of the wave motion is close to the profile of the 3rd harmonic, and this profile is fully located in the positive part of amplitudes. This unexpected picture is shown in Fig. 10.

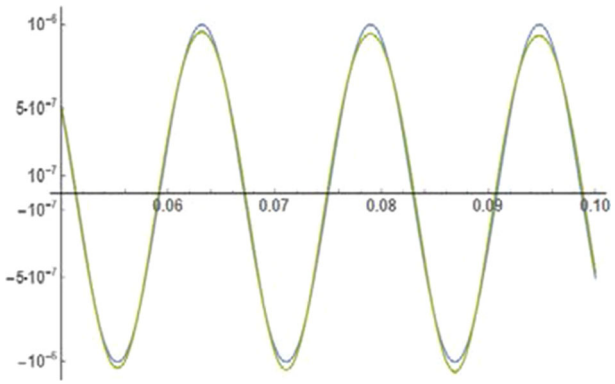

Fig. 7 Scenario cos + 0 + 1 + 2. Stage 1

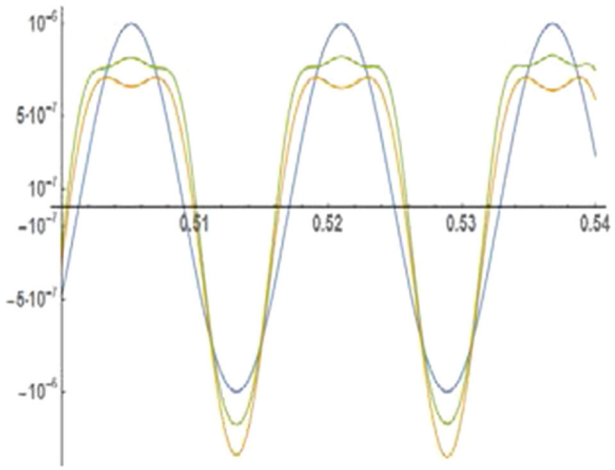

Fig. 8 Scenario cos + 0 + 1 + 2. Stage 2

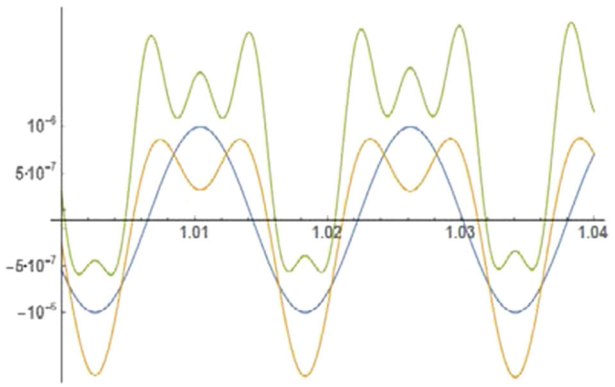

Fig. 9 Scenario cos + 0 + 1 + 2. Stage 3

Finally, some characteristic for the harmonic wave features of scenarios corresponding to the first two and first three approximations should be outlined.

Both cases are characterized by the graphs asymmetric relative to the horizontal axis and show the different speeds of evolution for positive and negative amplitudes.

In the case of a scenario cos + 0 + 1, the graphs go down, whereas in the case of the scenario cos + 0 + 1 + 2 the graphs go up. This shift in graphs corresponds to the phenomenon of lowering or raising the average value of the amplitude, relative to which oscillations occur. This can be seen in stages 3 and 4.

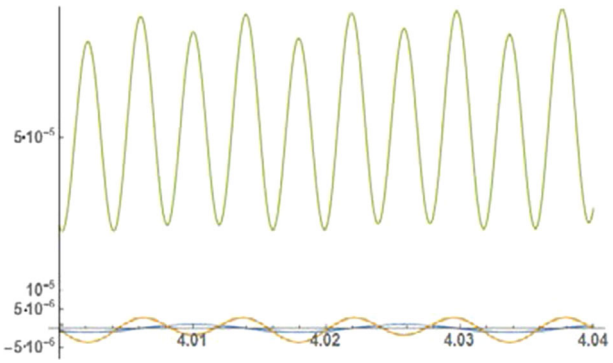

Fig. 10 Scenario cos + 0 + 1 + 2. Stage 4

In a certain approximation, Fig. 10 shows an increase in the average amplitude by the linear law. However, to manifest this phenomenon, the distances traveled by the wave must be large.

Thus, taking into account the 3rd approximation changes cardinally the scenario of the evolution of the harmonic wave.

3 Scenario of evolution of the solitary wave with initial profile in the form of Gauss function

The Gauss function has the form $F(x) = e^{-x^2/2}$ [20]. In the theory of waves, the wave with the initial profile in the form of Gauss function is often called the bell-shaped wave. The shape of such a wave

$$F(x_1) = e^{-\left[(a\,x_1)^2/2\right]} \tag{20}$$

is really like a bell shape.

If to analyse the solution of Eq. (6) in the form of the bell-shaped wave

$$u_1(x_1, t) = u_{1o}e^{-\left[a^2(x_1-vt)^2/2\right]} = u_{1o}e^{-\sigma^2/2} \tag{21}$$

and use the method of successive approximations, then the zeroth approximation has the form (21) where the unknown velocity v is changed on the known and constant c_L. The 1st approximation can be searched as the solution of an inhomogeneous equation [10, 11, 21, 22]

$$u^{(1)}_{1,tt} - (c_L)^2\, u^{(1)}_{1,11} = \left(N_1/\rho\right) u^{(0)}_{1,11}u^{(0)}_{1,1} \text{ or } u^{(1)}_{1,tt} - (c_L)^2\, u^{(1)}_{1,11} = \left(N_1/\rho\right)(u_{1o})^2a^3\sigma\left(1-\sigma^2\right)e^{-\sigma^2} \tag{22}$$

Because expression (21) is the solution of Eq. (22) corresponding to the homogeneous equation, then this solution should be represented to the form $u^{(1)}_1 = t\,A(\sigma)e^{-\sigma^2}$. The substitution of this representation into the left part of (22) and the change $B(\sigma) = t\,A(\sigma)e^{-\sigma^2}$ gives the inhomogeneous differential equation

$$\left[B''(\sigma) + 3\left(\sigma^2-1\right)B(\sigma)\right] = (u_{1o})^2\alpha a\sigma\left(1-\sigma^2\right)e^{\sigma^2/2} \tag{23}$$

The homogeneous equation $B''(\sigma) + 3\left(\sigma^2-1\right)B(\sigma) = 0$ corresponds to Eq. (11) from subsection (2.173) of [23] with $a = 0$, $b = 3$, $c = \sqrt{3}$ and can be reduced to the Whittaker equation. At that, a choice of the corresponding to the right-hand side of (22) partial solution seems very complicate owing presence of the factor $\sigma\left(\sigma^2-1\right)$. Thus, the 1st approximation will have a complicated mathematical form, which should still be found.

Most likely, the analytical and numerical analysis of wave evolution within the framework of the first two approximations will be looking very unpromising not only for the profile in the form of the bell-shaped function but for other solitary waves. In this situation, some advantage has the method of restriction on the gradient of displacement.

An important feature of this method [19, 21, 22] is that the studied nonlinear wave equation has a special structure: the right-side part of this equation can be carried over to the left-hand-side one and then formally the nonlinear equation can be written as the linear wave equation with the variable wave velocity.

In the case of Eq. (6), the appropriate form of the equation has the form

$$u_{1,\mathrm{tt}} - \left\{(c_L)^2 + \left(N_1/\rho\right)u_{1,1}\right\} u_{1,11} = 0 \rightarrow u_{1,\mathrm{tt}} - v^2 u_{1,11} = 0, v = c_L\sqrt{1+\alpha u_{1,1}}, \alpha = \left[N_1/(\lambda+2\mu)\right] \tag{24}$$

Further, the initial profile of wave is assumed to be the describing the waves arbitrary function $u(x_1, t = 0) == F(ax_1)$, where a is the arbitrary parameter characterizing the wavelength for harmonic waves and the wave bottom for solitary waves.

The wave is assumed to be propagated in the form

$$u(x_1, t) = F(\sigma), \tag{25}$$

where $\sigma = a(x_1 - vt)$ is the standard wave phase variable.

The restriction on the gradient of displacement $\left|\alpha u_{1,1}\right| \ll 1$ permits to represent approximately the velocity by only two first approximations $v = c_L\sqrt{1+\alpha\, u_{1,1}} \approx c_L\left[1 + \left(1/2\right)\alpha\, u_{1,1}\right]$. Then the phase can be approximately written in the form of two summands $\sigma \approx \left[a(x_1 - c_L t) - \left(1/2\right)\alpha a c_L u_{1,1} t\right]$. Now the solution can be represented also approximately in the form

$$u_1(x_1, t) \cong F\left[a\left(x_1 - c_L t - \left(1/2\right)\alpha c_L u_{1,1} t\right)\right] = F\left[a(x_1 - c_L t) - \left(1/2\right)\alpha a c_L u_{1,1} t\right] \tag{26}$$

The solution (26) can be expanded into the Taylor series by the small parameter $\left|\delta = -\left(1/2\right)\alpha a c_L u_{1,1} t\right| \ll 1$ within the neighborhood of the classical constant value $\sigma = a(x_1 - c_L t)$ and with saving only two first terms

$$u_{1,1}(x_1, t) \approx F'_\sigma(\sigma+\delta)\cdot\sigma'_{x_1} \approx aF'_\sigma(\sigma+\delta) \rightarrow F^{/}(\sigma+\delta) \approx F^{/}(\sigma) + F^{//}(\sigma)\delta$$

$$u_1(x_1, t) \approx F(\sigma) + F^{/}_{,1}(\sigma)a\delta = F(\sigma) - \left(1/2\right)\alpha a^2 c_L t\left[F^{/}_{,1}(\sigma)\right]^2 \tag{27}$$

The approximate representation (27) of the solution of the Eq. (24) takes into account the first two ap proximations and has a general character. It describes for different initial profiles $F(x_1)$ the same nonlinear effect—the initially linear form of solution (the conditional 1st harmonic) is complemented by the part of the solution generated by the nonlinearity of material (the conditional 2nd harmonics). From the point of view of wave mechanics, the presence of this new part means a distortion of the wave initial profile, because the value of this part is increased with time of wave propagation. In this way, the plane wave is evolved.

Because further the nonlinear wave Eq. (22) is solved within the framework of the first three approximations, then the shown above method should be extended on the case of allowance for the first three approximations.

In this case, three members instead of two should be saved in the approximate representation of the root $\sqrt{1+\alpha\, u_{1,1}} \approx 1 + \left(1/2\right)\alpha\, u_{1,1} - \left(1/8\right)\alpha^2\left(u_{1,1}\right)^2$. Then the wave velocity is now written takes the more complicate form $v = c_L\left[1 + \left(1/2\right)\alpha\, u_{1,1} - \left(1/8\right)\alpha^2\left(u_{1,1}\right)^2\right]$, and the approximate solution can be represented in a form that generalizes the corresponding representation (26)

$$u_1(x_1, t) \cong F\left\{a(x_1 - c_L t) - \left(1/2\right)t\alpha c_L u_{1,1}\left[1 - \left(1/4\right)\alpha u_{1,1}\right]\right\} \tag{28}$$

The following procedure is similar to the prior one—the smallness of the parameter δ^* should be assumed. $\left|\delta^* = -\left(1/2\right)t\alpha v_L u_{1,1}\left[1 - \left(1/4\right)\alpha u_{1,1}\right]\right| \ll 1$ and then the solution is decomposed into a Taylor series for a small parameter δ^* in the neighborhood of a phase value $\sigma = a(x_1 - c_L t)$

$$u(x_1, t) = F\left(\sigma + \delta^*\right) = F(\sigma) + F^{/}(\sigma)\delta^* + \left(1/2\right)F^{//}(\sigma)\delta^{*2} + \cdots \tag{29}$$

The final representation is obtained by saving only the first two members

$$\begin{aligned} u_1(x_1, t) &\approx F(\sigma) - F^{/}_{,1}(\sigma)a^2\left\{\left(1/2\right)t\alpha c_L F^{/}_{,1}(\sigma)\left[1 - \left(1/4\right)\alpha a F^{/}_{,1}(\sigma)\right]\right\} = \\ &= F(\sigma) - \left(1/2\right)\alpha a^2 c_L t\left[F^{/}_{,1}(\sigma)\right]^2\left[1 - \left(1/4\right)\alpha a F^{/}_{,1}(\sigma)\right]. \end{aligned} \tag{30}$$

Thus, the allowance for the 3rd approximation introduces new features in the scenarios 0 + 1 + 2 that are based on this approach. First of all, the representation (30) introduces asymmetric changes in the form of initial profile in contrary to the scenarios 0 + 1 which introduce the symmetric changes. Besides that, the representation (30) contains the 3rd approximation of cubic nonlinearity, which in the case of a harmonic

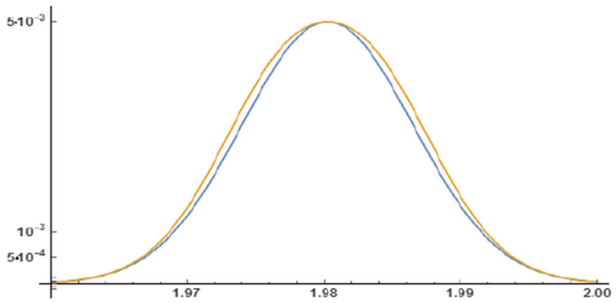

Fig. 11 Scenario Gauss + 0 + 1 + 2. Stage 1

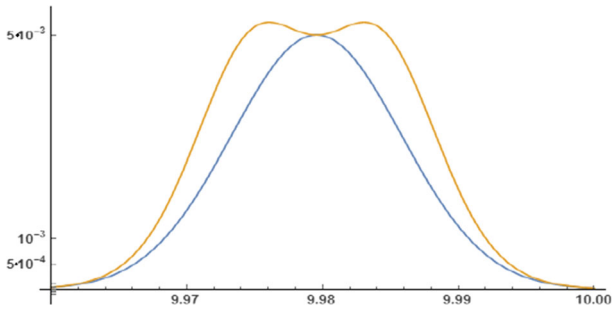

Fig. 12 Scenario Gauss + 0 + 1 + 2. Stage 2

profile means the presence of the 3rd harmonic in contrast to the effect of variant 7, where after the 2nd harmonic the 4th one is generated. But the Figs. 9 and 10 show that for sufficient long distances the harmonic wave if transformed just into the 3rd harmonic. Maybe, in both cases, the distance should be longer.

It seems to be important to note that the adequacy of approximate representation (30) depends on exactness of restriction on the parameter δ^* which includes wave velocity c_L, gradient of displacement $u_{1,1}$, and parameter $\alpha = 3 + 2(A + 3B + C)\big/(\lambda + 2\mu)$.

Consider at last the wave with the initial profile in the form $u_1(x_1, t) = u_{1o}e^{-\left[a^2(x_1 - vt)^2/2\right]} = u_{1o}e^{-\sigma^2/2}$ of Gauss function (21) and substitute the expression $F'_{,1}(\sigma) = \left(A^o e^{-\sigma^2/2}\right)_{,1} = -a\sigma A^o e^{-\sigma^2/2}$ into the general formula (30). Then the approximate solution of Eq. (24) can be written in the form

$$u_1(x_1, t) = A^o e^{-\sigma^2/2} - (1/2)t\alpha c_L a^2\sigma^2\left(A^o\right)^2 e^{-\sigma^2}\left[1 + (1/4)\alpha a v_L A^o \sigma e^{-\sigma^2/2}\right] =$$
$$= A^o e^{-\sigma^2/2} - (1/2)t\alpha c_L a^2\sigma^2\left(A^o\right)^2 e^{-\sigma^2} + (1/8)t\alpha^2 a^3 (v_L)^2\left(A^o\right)^3\sigma^3 e^{-3\sigma^2/2}. \quad (31)$$

If to assume that the expression $e^{-\sigma^2/2}$ is conditionally the first harmonic, then solution (31) includes the first three harmonics. The scenario Gauss + 0 + 1 + 2 is now described in the more complicated form as compared with the scenario Gauss + 0 + 1.

The scenarios of evolution Gauss + 0 + 1 and Gauss + 0 + 1 + 2 in three stages are shown in the next figures.

The Fig. 11 corresponds to the initial stage 1 and shows two lines. The internal line corresponds to the initial bell-shaped profile, and the external one corresponds to the first two and three approximations. This stage is characterized by the only tendency to an extension of the bell—it becomes wider and rests symmetric.

Stage 2 shows a tendency to formation two humps from one hump (two bells instead of one bell). This is looking very similar to the case of the harmonic profile when the 1st harmonic forms the plateau at the top and tends to the 2nd one. The maximal value of the amplitude is slowly increased for both new humps.

Stage 3 corresponds to the scenarios Gauss + 0 + 1 and Gauss + 0 + 1 + 2. The upper line in the left hump and lower line in the right hump correspond to scenario Gauss0 + 1 and shows some transformation of the symmetric profile into the asymmetric one (the left hump is higher than the left one). Whereas the scenario Gauss + 0 + 1 + 2 (the lower line in the left hump and upper line in the right hump) works oppositely—it tries to return the profile into the symmetric state. Thus, the allowance for the 3rd approximation changes very slightly the profile evolution that is formed by the first two approximations.

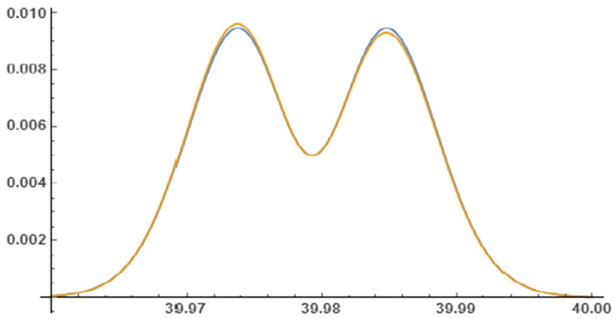

Fig. 13 Scenario Gauss + 0 + 1 + 2. Stage 3

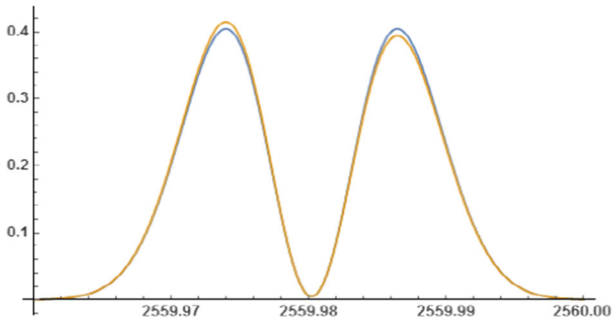

Fig. 14 Scenario Gauss + 0 + 1 + 2. Stage 4

The stage 4 corresponds to very long distance and is differing from the stage 3 by three new features—the maximal amplitudes of humps are decreased essentially, the allowance for the 3rd approximation generates new asymmetry (now the right hump is higher than the left one), the cavity between humps moves down and reach the common bottoms of the bells. At that, the graph does not cross the axis, dividing and splicing two humps. Also, the evolution of the initial symmetric relative to the vertical line profile generates the symmetric evolved profile on the whole. Nevertheless, is occurs asymmetrically relative to the peaks—from four sides of two humps, the outer sides (first and fourth) are more sloping.

Here, some similarities between scenarios for the harmonic and bell-shaped profiles can be seen—forming two humps instead of one hump. But on the whole, the difference is significant. For example, scenario Gauss + 0 + 1 + 2 shows the fission of one solitary wave on two solitary waves adjoining to each other.

4 Scenario of evolution of the solitary wave with initial profile in the form of Whittaker function

The Whittaker function $W_{k,m}(z)$ is a well-known mathematical function [24, 25]. It is defined for all values of indexes k, m, and all real nonnegative z. It can be presented on through a degenerate hypergeometric function $\Phi(a, c, z)$

$$W_{k,m}(z) = e^{-\frac{z}{2}} z^{m+\frac{1}{2}} \Phi\left(m - k + 1/2, 2m + 1, z\right) \tag{32}$$

The initial wave profile is chosen $F(x_1) = a_o W_{1/4;1/4}(x_1)$. The corresponding wave is assumed in the form

$$u_1(x_1, t) = a_o W_{1/4;1/4}(\sigma) \tag{33}$$

Further, the representation (33) should be substituted into the formula (30)

$$\begin{aligned} u_1(x_1, t) = a^o W_{1/4;3/4}(\alpha x_1) - \left(1/2\right) t\alpha c_L(a)^2 \left(a^o\right)^2 \left(W'_{1/4;1/4}(\alpha x_1)\right)^2 + \\ +(1/8) t(\alpha)^2 c_L(a)^3 \left(a^o\right)^3 \left(W'_{1/4;1/4}(\alpha x_1)\right)^3. \end{aligned} \tag{34}$$

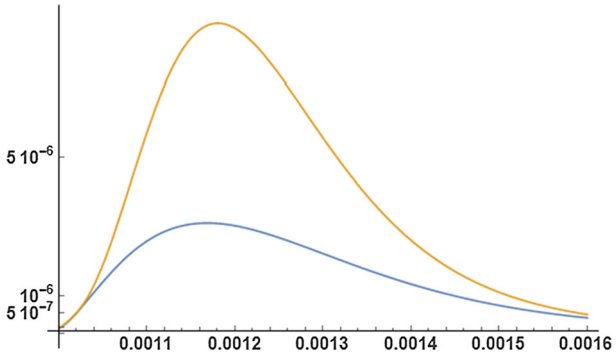

Fig. 15 Scenario Whittaker + 0 + 1 + 2. Stage 1

The formalism of obtaining the solution is the same as for the Gauss function. First, note that the derivative of the function $W_{\kappa,\mu}(z)$ is evaluated by the formula [24, 25]

$$\frac{d}{dz}W_{\lambda,\mu}(z) = \left(\frac{\lambda}{z} - \frac{1}{2}\right)W_{\lambda,\mu}(z) - \frac{1}{z}\left[\mu^2 - \left(\lambda - \frac{1}{2}\right)^2\right]W_{\lambda-1,\mu}(z) \tag{35}$$

and the first derivative for the function $W_{1/4;1/4}(x)$ has a form $\left(W_{1/4;1/4}(\sigma)\right)' = \left(\frac{5}{4\sigma} - \frac{1}{2}\right)W_{1/4,1/4}(\sigma)$. Then the solution (33) can be written as

$$\begin{aligned} u_1(x_1,t) = a^o W_{1/4;1/4}(\sigma) - (1/2)t\alpha c_L(a)^2(a^o)^2\left(\left(\frac{5}{4\sigma} - \frac{1}{2}\right)W_{1/4,1/4}(\sigma)\right)^2 + \\ +(1/8)t(\alpha)^2 c_L(a)^3(a^o)^3\left(\left(\frac{5}{4\sigma} - \frac{1}{2}\right)W_{1/4,1/4}(\sigma)\right)^3. \end{aligned} \tag{36}$$

Two evident features follow from the form of solution (36):

1. If conditionally the expression $a^o W_{1/4,1/4}(\sigma)$ is the 1st harmonic, then the solution (36) includes the first three harmonics. Note that the classical harmonics $\left\{e^{ikx}\right\}_{-\infty}^{+\infty}$ form the orthonormal system of functions, whereas the conditional harmonics of Gauss and Whittaker function don't form such a system.
2. This solution describes changing the initial profile of a solitary wave due to a direct dependence of the nonlinear components on time.

The resulting formula (36) can be used for the numerical simulation of the wave evolution. According to the formula (36), the two-dimensional graphs with coordinates "displacement u_1- wave propagation distance x_1" are built.

The Figs.15, 16, 17 correspond to the set of parameters which generates the very slow influence of nonlinearity and shows stage 1 only. Each figure contains two profiles. The wave bottom in all cases remains unchanged. The Fig. 15 shows the gently developed evolution of the initial profile. This profile is located closer to the abscissa axis. The upper profile corresponds to allowance for the first two approximations and the lower profile –(gently developed) (intermediately developed) to the first approximation. The main feature of this picture is that the maximal amplitude of evolved profile increases significantly. The profile rests asymmetric.

The Fig. 16 shows the intermediately developed evolution of the initial profile. Here, the quick decrease of the profile (moving down) is seen that corresponds to the first three approximations and is located lower of the profile corresponding to the first two approximations. The peak of the evolved profile is slightly moved to the ordinate axis. The profile rests asymmetric.

The Fig. 17 shows the well-developed evolution stage 1 of the initial profile. Here, the displayed in the prior step features are only developed.

The Figs.18, 19, 20 correspond to the set of parameters which generates the quite long influence of nonlinearity and shows three stages. Each figure contains two profiles. The wave bottom in all cases remains unchanged. The profile rests asymmetric. The stage of evolution in Fig. 18 is similar to the shown in Fig. 15.

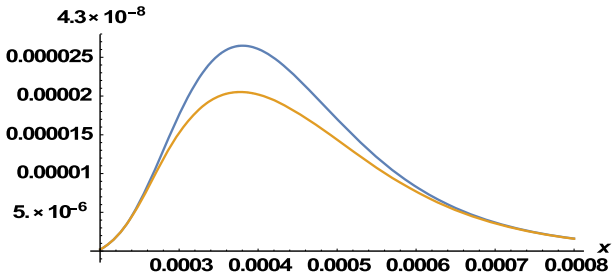

Fig. 16 Scenario Whittaker + 0 + 1 + 2. Stage 1

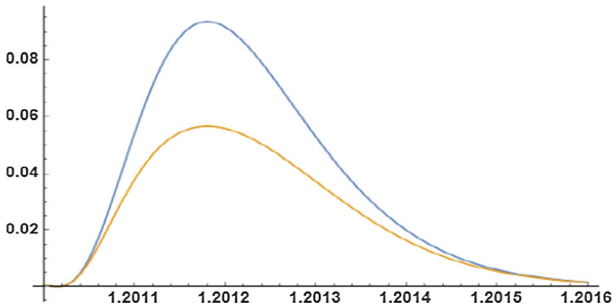

Fig. 17 Scenario Whittaker + 0 + 1 + 2. Stage 1 (well-developed)

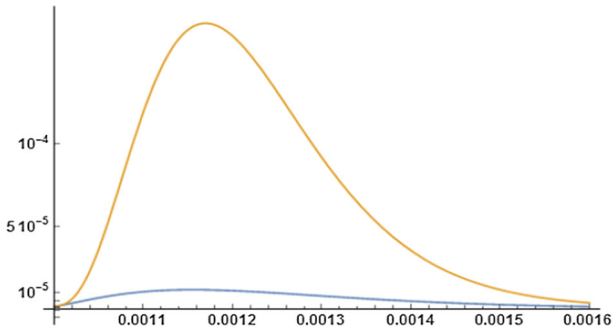

Fig. 18 Scenario Whittaker + 0 + 1 + 2. Stage 1

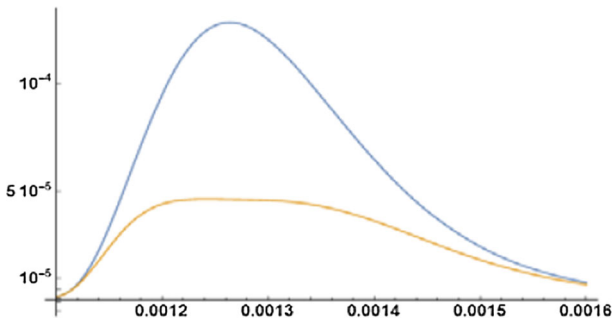

Fig. 19 Scenario Whittaker + 0 + 1 + 2. Stage 2

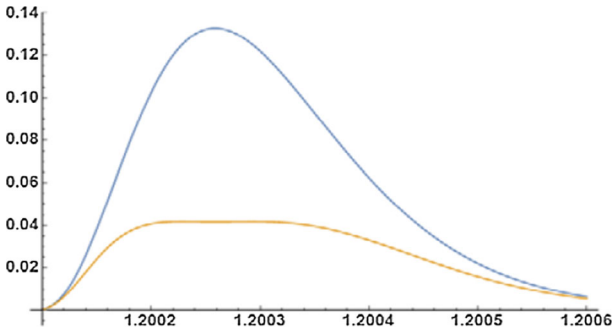

Fig. 20 Scenario Whittaker + 0 + 1 + 2. Stage 3

The Fig. 19 shows stage 2. Here, the tendency to forming the second hump can be seen. The cavity between humps appear. At that, the maximal amplitude of the evolved profile is decreased many times. Of course, this needs a long distance of propagation.

The Fig. 20 shows stage 3. Here, two equal by the shape humps appear and the cavity between humps is increased. These humps form the group which conditionally can be considered as the symmetric relative to the vertical line, but, on the whole, the evolved profile is asymmetric like the initial one. At that, the maximal amplitude of the evolved two-hump profile is continued to decrease.

Thus, the scenario Whittaker + 0 + 1 + 2 is quite new and not like the prior scenarios for other initial profiles. Nevertheless, it has some similar features with scenarios for the harmonic function and Gauss function. This is commented in the Conclusions.

5 Scenario of evolution of the solitary wave with initial profile in the form of Macdonald function

This wave is not the plane wave. It is one of the classical cylindrical waves. The case of a cylindrical radial wave of displacement is considered further which is described mathematically in the form very close to the used in the prior sections for the plane wave. In the linear theory of elasticity, such a wave is propagated in an infinite space with a cylindrical circular cavity. The motion of this wave in the radial direction is excited by a pulse applied to the boundary surface. In the simplest case, the impulse is uniform in space and harmonic in time. The cylindrical system of coordinates $Or\vartheta z$ is chosen in such a way that the Oz axis coincides with the axis of the cavity. Then the problem becomes the axisymmetric one and depending only on two variables—radius r and time t. The radial displacement u_r and three components of stress tensor $\sigma_{rr}, \sigma_{\vartheta\vartheta}, \sigma_{zz}$ only are non-zero. The linear motion equation has a form [10, 11, 21, 24]

$$\mu\left(u_{r,rr}+\frac{1}{r}u_{r,r}-\frac{u_r}{r^2}\right)+(\lambda+\mu)\left[\frac{1}{r}(ru_r)_{,r}\right]_{,r}-\rho u_{r,tt}=0 \tag{37}$$

The corresponding nonlinear equation within the framework of the Murnaghan model is as follows [10]

$$(c_L)^{-2}u_{r,tt}-\left(u_{r,rr}+\frac{u_{r,r}}{r}-\frac{u_r}{r^2}\right)=-\alpha_1 u_{r,rr}u_{r,r}-\alpha_2\frac{1}{r}u_{r,rr}u_r-\alpha_3\frac{1}{r^2}u_{r,r}u_r-\alpha_4\frac{1}{r}(u_{r,r})^2-\alpha_5\frac{1}{r^3}(u_r)^2 \tag{38}$$

$$\alpha_1=3+\frac{2(A+3B+C)}{\lambda+2\mu},\quad \alpha_2=\frac{\lambda+2B+2C}{\lambda+2\mu},\quad \alpha_3=\frac{\lambda}{\lambda+2\mu},$$

$\alpha_4=\frac{2\lambda+3\mu+A+2B+2C}{\lambda+2\mu}$, $\alpha_5=\frac{2\lambda+3\mu+A+2B+C}{\lambda+2\mu}$.

In the case when the solution of Eq. (38) is sought in the form of the harmonic in time wave of dis-placement the Eq. (38) can be considered as the nonlinear wave equation. The problem when the wave is propagated from the cylindrical cavity of the radius r_o and is excited by the harmonic in time displacement $u_r(r_o,t)=u_{ro}e^{i\omega t}$ or load $\sigma^{rr}(r_o,t)=p_o e^{i\omega t}$ is described in [10] by the method of successive approximations with taking into account the first two approximations. The linear (zeroth) approximation has a form

$$u_r^{(1)}(r,t)=u_r^o\,H_1^{(1)}(k_L r)e^{i\omega t}, \tag{39}$$

where the Hankel function of the first kind and first order is used and u_r^o is the amplitude factor.

$u_{ro} = -\frac{p_o k_L}{k_L(\lambda+2\mu)H_0^{1)}(k_L r_o) - \frac{2\mu}{r_o} H_1^{1)}(k_L r_o)}$.

The solution (39) shows that the wave is harmonic in time, and by the spatial coordinate is harmonic only asymptotically. The wave intensity decreases over time due to the properties of the Hankel function $H_1^{(1)}$. The 1st approximation was analyzed in different ways. The important conclusion from this analysis is that the four last nonlinear components in Eq. (38) with multipliers r^{-1}, r^{-2}, r^{-3} have little effect on the final result when increasing the distance from the cavity and analyzing the metallic engineering materials [10]. In other words, the defining nonlinear effect gives the term $\alpha_1 u_{r,rr} u_{r,r}$ and Eq. (38) can be simplified to the form

$$(c_L)^{-2} u_{r,tt} - \left(u_{r,rr} + \frac{u_{r,r}}{r} - \frac{u_r}{r^2}\right) = -\alpha_1 u_{r,rr} u_{r,r} \tag{40}$$

The stated above gives grounds for the following change in the initial nonlinear Eq. (38): save in the right-hand side of (38) expression $-\alpha_1 u_{r,rr} u_{r,r} - \alpha_3 \frac{1}{r^2} u_{r,r} u_r - \alpha_4 \frac{1}{r} (u_{r,r})^2$ and rewrite Eq. (38) in the form $u_{r,rr}\left(1 - \alpha_1 u_{r,r}\right) + \frac{1}{r} u_{r,r}\left(1 - \alpha_4 u_{r,r}\right) - \frac{u_r}{r^2}\left(1 - \alpha_3 u_{r,r}\right) - \frac{1}{(c_L)^2} u_{r,tt} = 0$. Then assume $\alpha_1 \approx \alpha_3 \approx \alpha_4$ and obtain finally the nonlinear wave equation

$$(c_L)^2\left(1 - \alpha_1 u_{r,r}\right)\left(u_{r,rr} + \frac{1}{r} u_{r,r} - \frac{u_r}{r^2}\right) - u_{r,tt} = 0 \tag{41}$$

In these circumstances, the equation that describes the cylindrical radial wave has the structure identical with the corresponding plane longitudinal wave—the homogeneous linear wave equation with the wave velocity nonlinearly depending on the solution.

Consider now Eq. (41) and assume the initial wave profile is described by the function $u_r(r, t = 0) = F(r)$

and the corresponding wave has the form

$$u_r(r, t) = u_r^o F(a(r - vt)) \tag{42}$$

where the unknown phase velocity is defined by the expression $v = \sqrt{1 - \alpha_1 u_{r,r}}\ c_L$ and u_r^o is the known constant initial amplitude coefficient.

Apply further the method of restriction on the gradient of displacement, assume $\left|\alpha_1 u_{r,r}\right| < 1$ and represent the root in the approximate form of the first three terms $\sqrt{1 - \alpha_1 u_{r,r}} \approx 1 - \left(1/2\right)\alpha_1 u_{r,r} + \left(1/8\right)(\alpha_1)^2 \left(u_{r,r}\right)^2$. Now the wave (42) can be represented approximately as follows

$$u_r(r, t) \cong u_r^o F\left[a(r - c_L t) - \left(1/2\right) a c_L \alpha_1 u_{r,r} t + \left(1/8\right) a c_L (\alpha_1)^2 \left(u_{r,r}\right)^2 t\right] \tag{43}$$

Now the expression (43) can be written in the form

$$u_r(r, t) = u_r^o F[a(r - vt)] = u_r^o F\left[a(r - c_L t) + \delta^*\right] = u_r^o F\left(\sigma + \delta^*\right) \tag{44}$$

where $\delta^* = -\left(1/2\right) a c_L \alpha_1 u_{r,r}\left[1 - \left(1/4\right)\alpha_1 u_{r,r}\right] t$ is the new parameter, which includes three known parameters —length of profile bottom a, wave velocity in the linear approach c_L, depending on properties of material parameter α_1—and the unknown gradient of displacement $u_{r,r}(r, t)$.

At this step, restrict the value of the new parameter

$$\left|\delta^* = -\left(1/2\right) a c_L \alpha_1 u_{r,r}\left[1 - \left(1/4\right)\alpha_1 u_{r,r}\right] t\right| < 1 \tag{45}$$

Note that the assumed before restriction $\left|\alpha_1 u_{r,r}\right| < 1$ and restriction (45) explain why the used here method is called the method of restriction on the gradient of displacement.

The introduced two restrictions permit to expand the solution (44) into the Taylor series by the small parameter (45) within the neighborhood of the classical value $\sigma = a(r - c_L t)$ with the constant wave velocity $c_L\ u_r(r, t) = u_r^o a F(\sigma + \delta^*) = u_r^o F(\sigma) + u_r^o F^{/}(\sigma)\delta^* + \left(1/2\right) u_r^o F^{//}(\sigma)\delta^{*2} + \cdots$ and saving only two first terms $u_r(r, t) = u_r^o F(\sigma + \delta^*) \approx u_r^o F(\sigma) + u_r^o F^{/}(\sigma)\delta^*$. The substitution into the last formula of the expression for the small parameter yields

$$u_r(r, t) \approx u_r^o F(\sigma) - \left(1/2\right) u_r^o F^{/}(\sigma) a c_L \alpha_1 u_{r,r}\left[1 - \left(1/4\right)\alpha_1 u_{r,r}\right] t \tag{46}$$

The differentiation of (42) gives the approximate formula $u_{r,r}(r,t) \cong u_r^o a F'(\sigma)$ which being substituted into the representation (46) gives the final approximate representation

$$u_r(r,t) \approx u_r^o F(\sigma) - \left(1/2\right)a^2\left(u_r^o\right)^2 c_L \alpha_1 t \left[F^{/}(\sigma)\right]^2\left[1 - \left(1/4\right)u_r^o a\alpha_1 F^{/}(\sigma)\right] \tag{47}$$

This representation includes three summands that can be treated as the first three approximations—the 1st corresponds to the linear approach, the 2nd introduces the quadratic nonlinear correction, the 3rd introduces the cubic correction to the linear approach. The same situation was seen in the corresponding formula for the plane waves. Note here once again that the application of the method of successive approximations introduces as the third approximation the correction of the fourth order, although the numerical modeling shows the third harmonic instead of the fourth one.

Consider now the case when the function $F[a(r - vt)]$ describes the solitary and not harmonic in time wave. Let us start with the linear approach. In this case, the corresponding to the nonlinear wave Eq. (40) linear wave equation

$$(c_L)^2\left(u_{r,rr} + \frac{1}{r}u_{r,r} - \frac{u_r}{r^2}\right) - u_{r,tt} = 0 \tag{48}$$

should be analyzed. The cylindrical function of the real argument—the Hankel function $H_\lambda(r)$—does not already the solution of this equation. But Eq. (48) has a solution in the form of the cylindrical function of the imagine argument—the Macdonald function $K_\lambda(r)$ [20, 25].

Choose the initial profile in the form of the function $F(\sigma) = K_0(\sigma)$ and substitute this concrete expression into the formula (47)

$$u_r(r,t) \approx u_r^o a K_0(\sigma) - \left(1/2\right)a^3\left(u_r^o\right)^2 c_L \alpha_1 t \left[K_0^{/}(\sigma)\right]^2\left[1 - \left(1/2\right)u_r^o \alpha_1 a K_0^{/}(\sigma)\right] \tag{49}$$

Use the known formula [20, 25] $K_0^{/}(\sigma) = -K_1(\sigma)$ and transform the approximate representation of the nonlinear wave into the new form

$$u_r(r,t) \approx K_0(a(r - c_L t)) - \left(1/2\right)a^3\left(u_r^o\right)^2 \alpha_1 a c_L t[K_1(a(r - c_L t))]^2\left[1 + \left(1/4\right)u_r^o \alpha_1 a K_1(a(r - c_L t))\right] \tag{50}$$

This formula includes the first three approximations.

Two evident features follow from the form of solution (50): 1.This solution describes changing the initial pro file of a solitary Macdonald wave due to a direct dependence of the nonlinear components on time. 2.The shapes of Macdonald's functions plots are that they have any humps and like to the hyperbola. Therefore, it is unlikely to expect the appearance of some humps. The distorted profile will be probably smooth and repeat the initial profile shape. 3. Because the plots of Macdonald functions are very similar and become less steep with increasing the index of function, then the distorted profile (50) will be also less steep as compared with the initial one.

The resulting formula (50) can be used for the numerical simulation of the wave evolution. According to this formula, the two-dimensional graphs with coordinates "displacement u_r- wave propagation distance r" are built. They show the scenario very dinstinguishing from the scenarios for the analyzed before cosinus, Gauss, Whittaker profiles.

The Fig. 21 corresponds to stage 1, when nonlinearity has a small effect on the evolution. The left line corresponds to the linear (zeroth) approximation, and the right line—to the 0 + 1 approximation. Thus, the distorted profile becomes gently steeper and shifted to the right side from the initial profile. The bottom of the distorted profile is shortened.

The Fig. 22 shows the more developed evolution of the initial profile (the 45 times longer distance of propagation) and corresponds to stage 2. It saves the displayed in stage 1 features. The distorted profile becomes steel more steep and still more shifted to the right side from the initial profile. The bottom of the distorted profile is still more shortened.

The Fig. 23 shows the more developed evolution of the initial profile (the 70 times longer distance of pro pagation) and corresponds to stage 3. It also saves the displayed in stages 1 and 2 features. The distorted profile becomes still steeper and still more shifted to the right side from the initial profile. The bottom of the distorted profile is continued to shorten.

The Fig. 24 compares the first two approximations and the first three approximations. It shows two lines. The left line corresponds to the 0 + 1 approximation, and the right line corresponds to the 0 + 1 + 2 approximation.

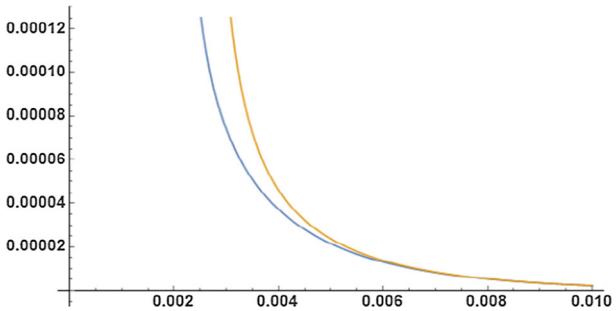

Fig. 21 Scenario Macdonald + 0 + 1. Stage 1

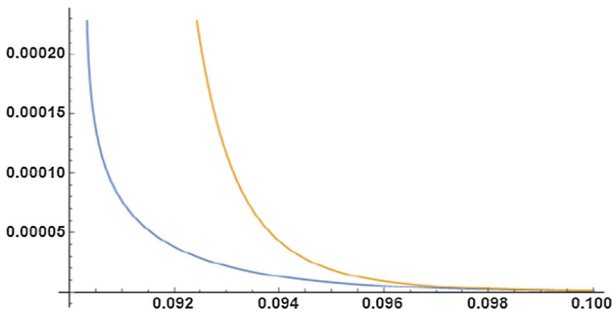

Fig. 22 Scenario Macdonald + 0 + 1. Stage 2

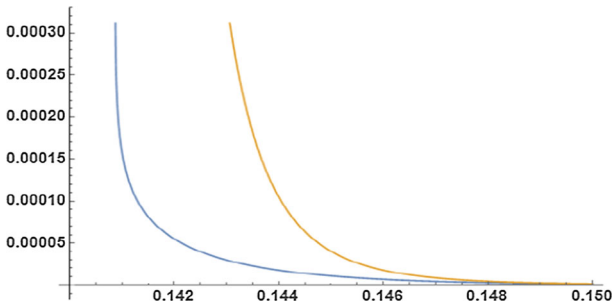

Fig. 23 Scenario Macdonald + 0 + 1. Stage 3

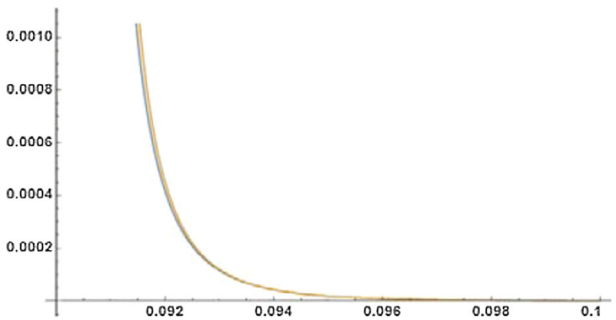

Fig. 24 Scenario Macdonald + 0 + 1 + 2. Stage 1

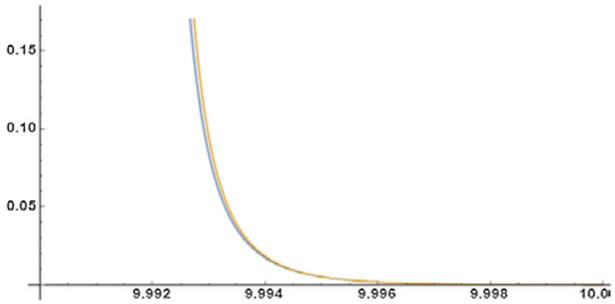

Fig. 25 Scenario Macdonald + 0 + 1 + 2. Stage 2

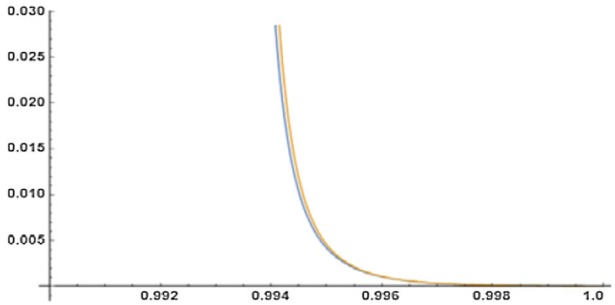

Fig. 26 Scenario Macdonald + 0 + 1 + 2. Stage 2

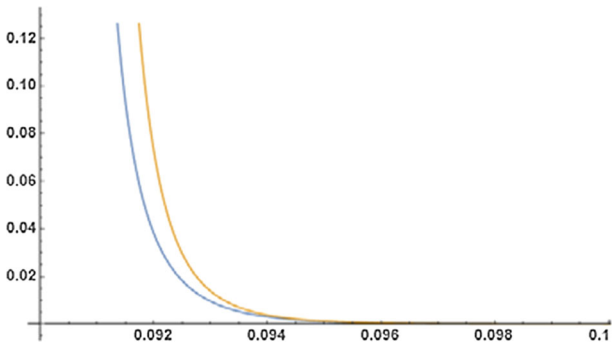

Fig. 27 Scenario Macdonald + 0 + 1 + 2. Stage 1 +

The Figs.25 and 26 compare the profiles within the framework of the first two approximations and the first three approximations for the case of the longer ten times distance of wave propagation. This comparison testifies that for the standard set of parameters the third approximation introduces the small contribution. Thus, the increase in the distance of wave propagation will increase the effect shown in stage 2.

The Figs. 27, 28, 29 show the more developed evolution for the 0 + 1 + 2 approximation. By the structure, these figures repeat the last three figures. But since the numerical modeling includes three important parameters of the problem, and it is known that an increase of the initial profile amplitude accelerates the evolution, then Figs. 27, 28, 29 are specially built for the ten times more initial profile amplitude.

As it follows from these figures, the effect of the 3rd approximation is more visible and tangible.

6 Conclusions

The considered four waves with the initial profiles in the form of cosinusoidal, Gauss, Whittaker, Macdonald functions show the distinguishing scenarios of evolution while being propagated in the same nonlinear elastic material. Despite that two first profiles have initially the symmetric shape and the two last are nonsymmetric, some similar features in scenarios can be seen, but in many features, the scenarios are not similar. The main similarity for the first three profiles is that initially one-hump shape is transformed into the two-hump one and

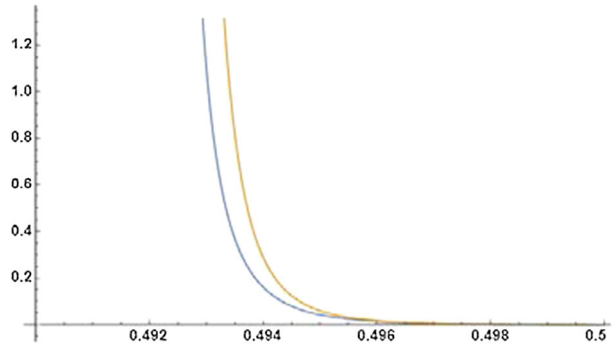

Fig. 28 Scenario Macdonald + 0 + 1 + 2. Stage 2 +

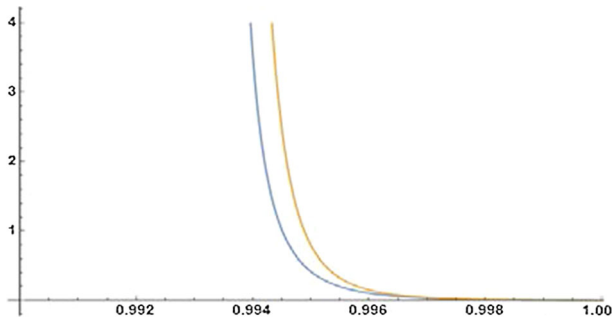

Fig. 29 Scenario Macdonald + 0 + 1 + 2. Stage 2

even for the long distances of propagation two-hump shape can be transformed into the many-hump one. The second kind of similarity is that all symmetric shapes are formed with time into the nonsymmetric ones both relative the horizontal line of symmetry and for the vertical line.

The Macdonald profile is quite different. Along all stages of the scenario, it rests smoothly and sloping. It is distorted in three directions—it becomes steeper and steeper, shifted to the right side from the initial profile, and its bottom is smaller and smaller. The last conclusion is that the allowance for the third approximation gives new information on scenarios of propagation of solitary waves.

References

1. Riemann, B.: Über die Fortpflanzung ebener Luftwellen von endlichen Schwingungsweite (On propagation of plane air wave with finite amplitude oscillations). Abhandlungen der Königischen Gesellschaft zu Göttingen, Bd VIII, S.43 (1860) In: Bernhards Riemann's gesammelte mathematische Werke und Wissen- schaftlicher Nachlass, 2-te Auflage. Teubner Verlag, Leipzig, S.157–179 (1892) In: B.Riemann Gesam- melte mathematische Werke, wissenschaflicher Nachlass und Nachtrage. Collected papers. Springer Ver- lag/Teubner Verlaggesellschaft, Berlin-Leipzig (1990)
2. Whitham, J.: Linear and Nonlinear Waves. Wiley, New York (1974)
3. Lighthill, M.J.: Waves in Fluids. Cambridge University Press, Cambridge (1978)
4. Maugin, G.A.: Continuum Mechanics of Electromagnetic Solid. North Holland, Amsterdam (1988)
5. Maugin, G.: Nonlinear Waves in Crystals. Oxford University Press, Oxford (1999)
6. Murnaghan, F.: Finite Deformation in an Elastic Solid, 2nd edn. Wiley, New York (1967)
7. Guz A.N.: Elastic waves in bodies with initial stresses. In 2 vols. Vol.1. General problems. Vol.2. Propagation regularities. Naukova Dumka, Kiev (1986) (**In Russian**)
8. Hauk, V.: Structural and Residual Stress Analysis. Elsevier, Amsterdam (2006)
9. Lur'e, A.: Nonlinear Theory of Elasticity. North-Holland. Amsterdam (1990)
10. Rushchitsky, J.: Nonlinear Elastic Waves in Materials. Series: Foundations of Engineering Mechanics. Springer, Heidelberg (2014)
11. Cattani, C., Rushchitsky, J.: Wavelet and Wave Analysis as Applied to Materials with Micro and Nano- Structure. Series on Advances in Mathematics for Applied Sciences. World Scientific, Singapore (2007)
12. Zarembo, L.B., Krasilnikov, A.V.: Introduction to Nonlinear Acoustics. Moscow University Press, Mos- cow (1966).. ((**In Russian**))
13. Bloembergen, N.: Nonlinear optics a lecture note. W.A. Benjamin Inc., New York (1965)
14. Yariv, A.: Quantum Electronics. Wiley, New York (1967)

15. Rushchitsky, J.: Self-switching of displacement waves in elastic nonlinearly deformed materials. Comptes Rendus de l'Academie des Sci. Serie IIb Mecanique. **330**(2), 175–180 (2002)
16. Rushchitsky, J.J.: On the self-switching of hypersonic waves in quadratically nonlinear elastic nanocom-posites. Int. Appl. Mech. **45**(1), 73–93 (2009)
17. Rushchitsky, J.J.: Features of development of theory of elastic nonlinear waves. Math. Methods Phys. Mech. Fields. **46**(3), 90–105 (2009)
18. Rushchitsky, J.J., Sinchilo, S.V., Khotenko, I.N.: On generation of the second, fourth, eighth and follow-ing frequencies of quadratically nonlinear hyperelastic plane longitudinal wave. Int. Appl. Mech. **46**(6), 90–98 (2010)
19. Rushchitsky, J.J.: Plane Nonlinear ElasticWaves: ApproximateApproachestoAnalysis of Evolution. In: Cooper, W.A. (ed.) Cha-pter 3 in the book "Understanding Plane Waves, pp. 58–80. Nova Science Publishers, London (2019)
20. Gradstein, I., Ryzhik, I.: Table of Integrals series and products, 7 revised Academic Press Inc., New York (2007)
21. Rushchitsky, J.J., Yurchuk, V.N.: An approximate method of analysis of solitary waves in materials defo- rming elastic nonlinearly. Int. Appl. Mech. **52**(3), 282–289 (2016)
22. Rushchitsky, J.J., Yurchuk, V.N.: Numerical analysis of the evolution of plane longitudinal nonlinear elas- tic waves with different initial profiles. Int. Appl. Mech. **53**(1), 104–110 (2017)
23. Kamke, E.: Differentialgleichungen. Lösungmethoden und Lösungen. (Differential Equations. Methods of Solving and Solutions). Vieweg+Teubner Verlag, Springer Fachmedien Wiesbaden GmbH, Wiesbaden (1977)
24. Olde Daalhuis, A.: Confluent Hypergeometric Functions. Whittaker Functions. Chapter 13. In: Olver, F.W.J., Lozie, D.W., Bousvert, R.F., Clark, C.W. (eds.) Handbook of mathematical functions. NIST National Institute of Standards and Technology, Cambridge University Press, Cambridge (2010)
25. Whittaker, E.T., Watson, G.N.: A Course of Modern Analysis an Introduction to the General Theory of Infinite Processes and of AnalyticFunctions; with an Account of the PrincipalTranscendentalFunctions, 4th edn. Cambridge University Press, Cambridge (1927)